

Self-Organized Hierarchical ZnS/SiO₂ Nanowire Heterostructures

Guozhen Shen,* Yoshio Bando, Chengchun Tang, and Dmitri Golberg

Advanced Materials Laboratory, National Institute for Materials Science (NIMS),
Namiki 1-1, Tsukuba, Ibaraki 305-0044, Japan

Received: January 1, 2006; In Final Form: February 23, 2006

Novel hierarchical heterostructures formed by wrapping ZnS nanowires with highly dense SiO₂ nanowires were successfully synthesized by a vapor–liquid–solid process. The as-synthesized products were characterized using X-ray diffraction, scanning electron microscopy and transmission electron microscopy equipped with an energy-dispersive X-ray spectrometer. Studies indicate that a typical hierarchical ZnS/SiO₂ heterostructure consists of a single-crystalline ZnS nanowire (core) with diameter gradually decreasing from several hundred nanometers to 20 nm and adjacent amorphous SiO₂ nanowires (branches) with diameters of about 20 nm. A possible growth mechanism was also proposed for the growth of the hierarchical heterostructures.

Introduction

In recent years, great efforts have been paid to the synthesis and characterization of nanoscale materials as well as devices fabricated from them.^{1–3} Manipulation with a given nanoscale object presumes not only the generation of pure nanomaterials with novel properties, but also the realization of multicomponent nanosystems (heterostructures) with diverse functions. One-dimensional (1-D) heterostructures with modulated compositions and interfaces are of particular interest with respect to the potential applications in unique types of nanoscale building blocks for future optoelectronic devices and systems.⁴ However, compared with the significant progress in the fabrication of homogeneous 1-D nanostructures (nanotubes, nanowires, and nanobelts),^{5–12} the formation of 1-D heterostructures with well-defined interfaces and compositions has been lingering far behind. To date, only several works have been successfully completed on 1-D heterostructures, e.g., superlattice nanowires, core–sheath coaxial nanowires, nanotypes, and metal–insulator nanocables.^{13–18}

Very recently, complex 1-D hierarchical heterostructures have attracted considerable attention. For example, ZnO based hierarchical heterostructures, such as In₂O₃/ZnO heterostructures with different symmetries, GaP/ZnO, SiC/ZnO, and GaN/ZnO heterostructures, etc, have been explored by several groups.¹⁹ The fabrication of hierarchical heterostructures consisted of Si microwires (core) and SiO₂ nanowires (branches), as well as the ZnS/BN heterostructures, were also reported.²⁰

In this paper, we report on the fabrication of novel ZnS/SiO₂ hierarchical heterostructures via a high-temperature vapor–liquid–solid process (VLS). In the typical synthesis, a mixture of commercial ZnS, SiO, and GaN powders was used as the precursor, and Ar gas was used as the carrier and protective gas. The synthesized ZnS/SiO₂ hierarchical heterostructures were composed of single-crystal ZnS nanowires (core) wrapped with high-density SiO₂ nanowires (branches).

Experimental Section

The ZnS/SiO₂ materials were synthesized in a vertical induction furnace, as described in detail in ref 21. The furnace

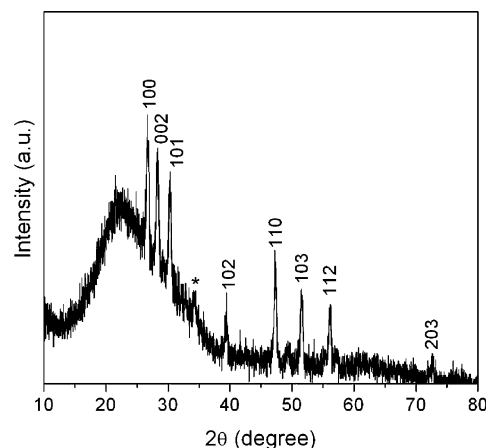


Figure 1. XRD pattern of a product.

consisted of a fused-quartz tube and an induction-heated cylinder made of high-purity graphite coated with a carbon fiber thermo-insulating layer. The furnace had two inlets on its top and base, respectively, and an outlet on its base. A graphite crucible, containing a mixture of ZnS (0.49 g), SiO (0.8 g), and GaN (0.1 g) powders, was placed at the center cylinder zone. After evacuation of the quartz tube to ~20 Pa, two pure Ar flows were introduced into the furnace through the inlets at the top and base, respectively, which were maintained at a constant flow rate of 400 sccm (top) and 600 sccm (base), respectively. The furnace was rapidly heated and kept at 1350 °C for 1h. After the reaction was terminated and the system cooled to room temperature, the collected products were characterized using powder X-ray diffraction (RINT 2200HF), scanning electron microscopy (SEM, JSM-6700F), and a transmission electron microscope (HRTEM, JEM-3000F) equipped with an energy-dispersive X-ray spectrometer (EDS).

Results and Discussion

After synthesis, the gray–yellow colored product was found on the inner wall of the graphite crucible. The yield of the product is ~15% based on the amount of ZnS used. Figure 1 shows the typical XRD pattern of the obtained product. All the strong peaks in this pattern can be readily indexed to hexagonal

* To whom correspondence should be addressed. E-mail: SHEN.Guozhen@nims.go.jp. Fax: + 81-29-851-6280.

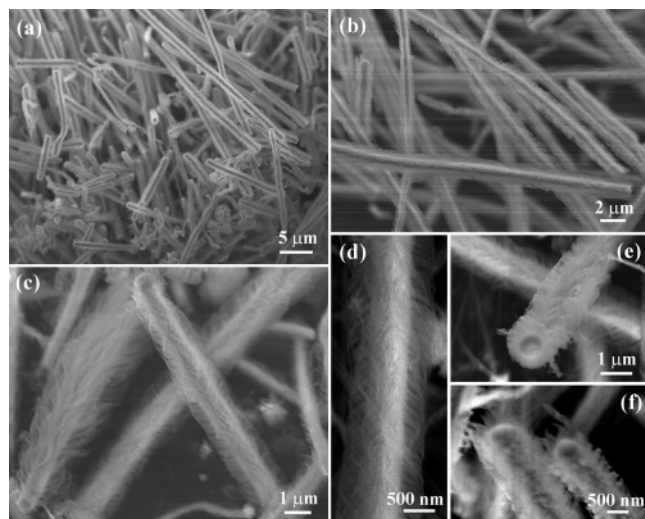


Figure 2. SEM images of hierarchical ZnS/SiO₂ nanostructures, which are composed of ZnS core nanowires wrapped with high-density SiO₂ nanowires.

wurtzite ZnS structures. The peak marked with a star comes from metallic Ga. Besides the strong diffraction peaks, a broad peak located at $\sim 23^\circ$, which indicates that there are some amorphous materials in the product.

Figures 2a and 2b are scanning electron microscopy (SEM) images, which show the general morphology of the product. From these images, it can be seen that the products possess interesting hierarchical “leaf-like” structures. Typical structures have mean diameters of about 1–2 μm and lengths ranging from several to several tens micrometers. High-magnification SEM images shown in Figure 2c and d indicate that each structure consists of a main stem with diameter of several tens to several hundred nanometers and numerous aligned, close-packed small-diameter branches. During SEM observations, it was found that there are spherical particles attached to the most of structure tip-ends, as shown in Figure 2e and f. This indicates that the structure formation may follow the VLS mechanism. Energy-dispersive X-ray spectrometer (EDS) and selected area electron diffraction (SAED) analysis reveal that the core stems are made of single-crystal ZnS nanowires, whereas the outer branches are composed of amorphous SiO₂ nanowires (see the following discussions). Therefore, the present nanostructures may be generally classified as core–shell ZnS–SiO₂ heterostructures.

The structures and morphologies of the hierarchical core–shell ZnS–SiO₂ heterostructures were further characterized using transmission electron microscopy (TEM). Figure 3a shows the TEM image of several leaf-like structures, in accord with the SEM observations. The branched SiO₂ nanowires have mean diameters of about 20 nm and lengths of 100–200 nm. In fact, the core ZnS nanowire stems in the synthesized structures have diameters gradually decreasing from about 200–500 nm in the tips to 50 nm in the bottoms, rather than constant diameters along the whole length. Figure 3b clearly shows a hierarchical leaf-like structure with a core ZnS nanowire with diameter gradually decreasing along its axis. Hierarchical leaf-like structures with the core partially filled with ZnS nanowires were also observed, as shown in Figure 3c. SAED pattern recorded from the branches (Figure 3d) shows only diffusive rings, indicating the amorphous state of the branch’s nanowires. Figure 3e is a SAED pattern recorded from the core nanowire. It shows intense diffraction spots, implying the single-crystal nature of the core nanowires.

Figure 4a shows the TEM image of a typical hierarchical ZnS/SiO₂ heterostructure fragment. The corresponding high-

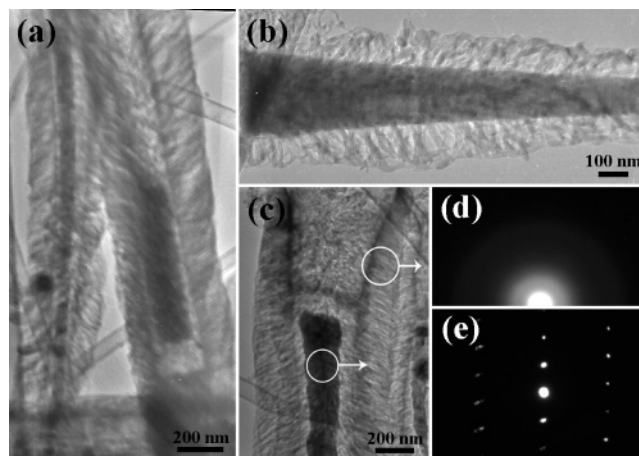


Figure 3. (a,b) Typical TEM images of the ZnS/SiO₂ hierarchical nanostructures; (c) TEM image of a partly filled hierarchical nanostructure; (d) SAED pattern taken from the SiO₂ nanowires; (e) SAED pattern taken from the ZnS nanowires

resolution TEM (HRTEM) image recorded from the joint part of the core ZnS nanowire and the branched SiO₂ nanowire is shown in Figure 4b. The HRTEM image clearly shows that the branched SiO₂ nanowires are amorphous, while the core ZnS nanowires are single crystalline. The observed inter-planar d spacing is 0.31 nm corresponds well with that of the [0001] lattice plane spacing of wurtzite ZnS. EDS spectra recorded from both the core single crystalline nanowire and the branched amorphous nanowires further verify the structure chemical composition. The spectra (Figures 4c and d) show the appearance of Zn and S X-ray signals for the core single crystalline nanowire and Si and O reflections for the branched amorphous nanowires, thus confirming that the crystalline nanowire is made of ZnS, and the branched amorphous nanowires are composed of SiO₂.

Since at least one of the two ends of the present leaf-like structure is opened, the inner ZnS nanowires can be easily removed by hydrochloric acid treatment. Figure 5a shows the SEM image of the product after hydrochloric acid treatment. It can be seen that the inner ZnS nanowires have been completely removed and only one-dimensional hollow SiO₂ structures with numerous nanowire branches along the growth length are left. A high-magnification SEM image in Figure 5b clearly reveals the remained hollow SiO₂ structure. The hollow structures were also characterized using TEM analysis. TEM images shown in Figures 5c and d also confirm the completed removal of ZnS nanowires.

In the present synthetic process, gallium nitride plays an important role in the nanostructure formation. The synthesized wires were capped with spherical particles, which is the key feature of the VLS growth mechanism. Most importantly, in the absence of GaN, no heterostructures can be obtained; only ZnS nanoparticles and a few Si nanowires form. At high temperature, GaN will thermally decompose to generate Ga vapors, which are transferred to the low temperature regions and deposit at the inner wall of the graphite crucible in the form of Ga droplets. The decomposition of GaN at high temperature was confirmed by the fact that a lot of Ga droplets remained in the crucible after reaction. High temperature is obviously not suitable for the formation of the present nanostructures since no product remained in the reaction system.

Vapor–solid and vapor–liquid–solid (VLS) mechanisms have been widely used to explain the formation of one-dimensional structures.²² During the SEM observations, it was

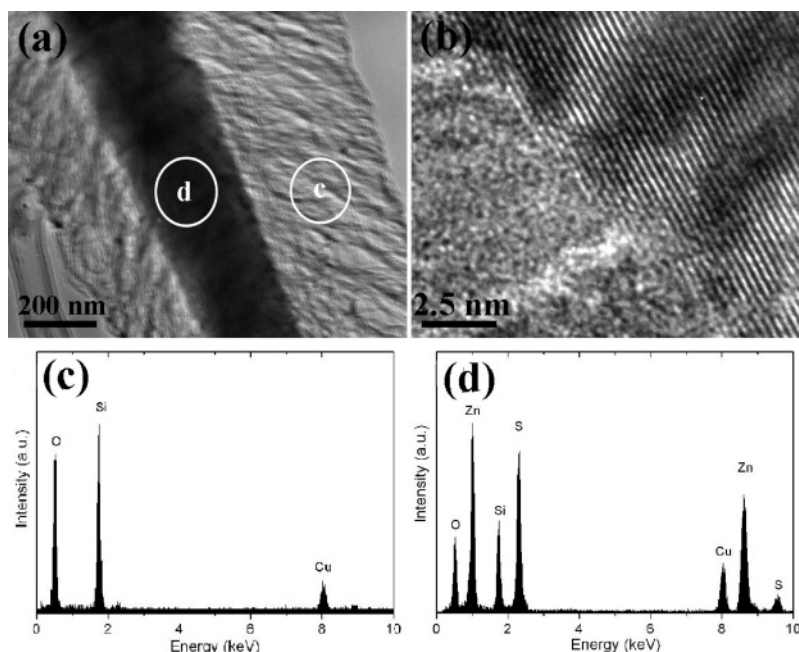


Figure 4. (a) TEM image of the ZnS/SiO₂ hierarchical nanostructures; (b) HRTEM image taken from the joint part a ZnS nanowire and a SiO₂ nanowire; (c,d) EDS spectra taken from the shell and the core parts marked in Figure 4a, respectively.

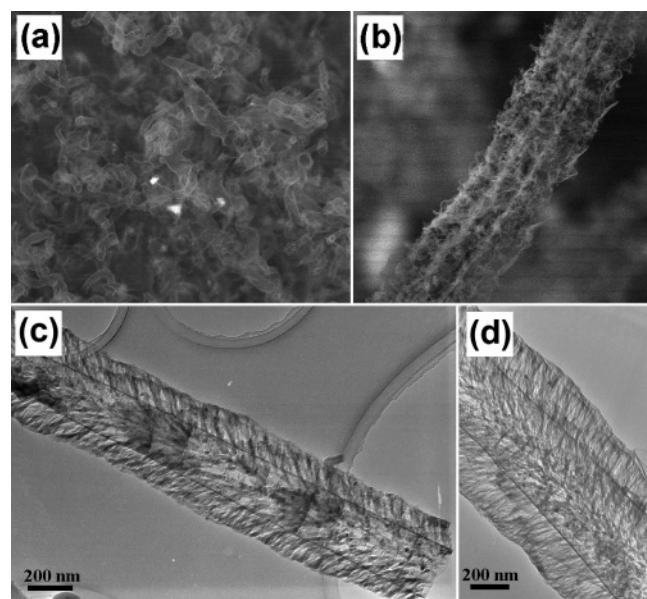


Figure 5. TEM images of the hollow SiO₂ nanostructures after hydrochloric acid treatment

found that there are spherical particles attached to the tips of most of the present ZnS/SiO₂ heterostructures. This implies that their formation may follow the VLS mechanism. Besides the formation of hierarchical structures, some amorphous SiO₂ nanotubes and ZnS/SiO₂ nanocables were found in the product (Figure 6). Both the SiO₂ nanotubes and the ZnS/SiO₂ nanocables have similar dimensions with those of the core ZnS nanowires in the hierarchical heterostructures, implying that those SiO₂ nanotubes and the ZnS/SiO₂ nanocables may represent the intermediate state of the final morphology.

Based on all the above analysis, we deduce the possible formation mechanism (Figure 7). A GaN powder thermally decomposes at a high temperature to generate Ga; the newly formed Ga may be in the form of clusters. These Ga clusters are then transported by the Ar gas to the low temperature furnace zone, where they deposit on the inner wall of graphite crucible in the form of small droplets (Figure 7I). These small droplets

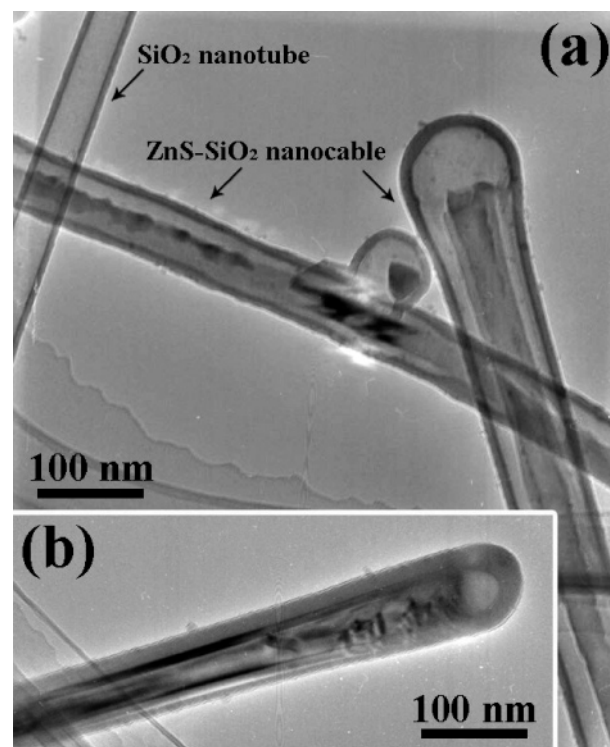


Figure 6. (a) TEM image of the SiO₂ nanotubes and ZnS-SiO₂ nanocables; (b) TEM image of a typical ZnS-SiO₂ nanocable. The SiO₂ nanotubes and ZnS-SiO₂ nanocables coexist with the ZnS/SiO₂ heterostructures and their dimensions are similar with the ZnS/SiO₂ heterostructures.

are energetically favored sites for the absorption of incoming ZnS vapors. The process leads to the formation of Zn-S-Ga alloys (Figure 7II). With the gradual absorption of ZnS vapors, the Zn-S-Ga alloys become supersaturated and one-dimensional ZnS nanowires form (Figure 7III). Thermal deposition of SiO at a high temperature results in the generation of Si vapors, which are rapidly oxidized to SiO_x by the residual or leaking oxygen. The SiO_x vapors are also transported by the carrier gas to the low-temperature zone where they deposit on

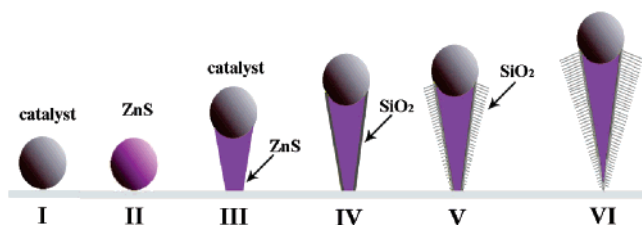


Figure 7. Schematic illustration of the formation of hierarchical ZnS/SiO₂ nanostructures via a Ga-catalyzed vapor-solid-liquid process. (I) Formation of liquid-Ga droplets; (II) condensation of ZnS on Ga droplets; (III) simultaneous growth of ZnS nanowires; (IV) formation of ZnS/SiO₂ nanocables; (V,VI) growth of hierarchical ZnS/SiO₂ heterostructures.

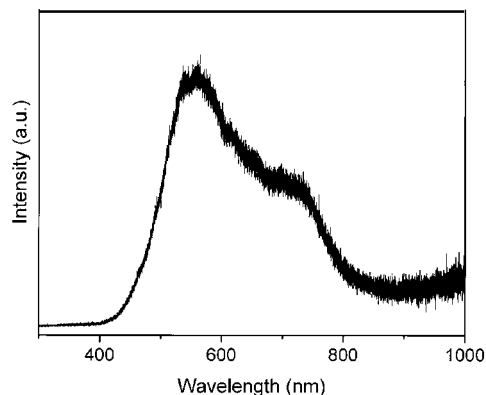


Figure 8. Room-temperature PL spectrum of the hierarchical ZnS/SiO₂ nanostructures.

the ZnS nanowire surfaces to form ZnS/SiO₂ nanocables (Figure 7IV). Gradual absorption of SiO_x causes the epitaxial growth of SiO₂ nanowires on the nanocables (Figure 7V) and, finally, leads to the formation of hierarchical ZnS/SiO₂ heterostructures (Figure 7VI). A similar mechanism has been used to explain the growth process of highly aligned silica nanowires.²³

Figure 8 shows the room-temperature photoluminescence (PL) properties of the synthesized hierarchical ZnS/SiO₂ nanostructures measured using a He–Cd laser line at 325 nm as the excitation source. The spectrum shows a strong emission at about 558 nm and a weak emission at about 720 nm. The emission at 558 nm may originate from some self-activated centers, vacancy states, element sulfur species on the ZnS surface, or interstitial states associated with the peculiar nanostructures according to the previous reports.²⁴ Due to the special complex structures, some defects, other than Schottky vacancy defects, may be present in the hierarchical ZnS/SiO₂ nanostructures, which can be used to explain the low-energy emission at 720 nm.

Conclusion

In conclusion, hierarchical ZnS/SiO₂ heterostructures have been self-organized via a high-temperature vapor–liquid–solid process using a mixture of ZnS, SiO, and GaN powders as the source material. Studies indicate that typical hierarchical ZnS/SiO₂ heterostructure consists of a single-crystalline ZnS nanowire (core) with diameter gradually decreasing from several hundred nanometers to 20 nm and adjacent amorphous SiO₂ nanowires (branches) with diameters of about 20 nm. This technique is also useful for the fabrication of heterostructures of other materials, for example, CdS/SiO₂ heterostructures, Zn₃P₂/ZnS heterostructures, etc.

Acknowledgment. We thank Dr. J. Q. Hu, K. Kurashima, Y. Uemura, and Dr. C. Y. Zhi, for helpful discussions. We also

thank Dr. D. Chen at University of Science and Technology of China for PL measurement.

References and Notes

- (1) (a) Manna, L.; Scher, E. C.; Alivisatos, A. P. *J. Am. Chem. Soc.* **2000**, *122*, 12700. (b) Peng, Z. A.; Peng, X. G. *J. Am. Chem. Soc.* **2002**, *124*, 3343. (c) Ma, D. D. D.; Lee, C. S.; Au, F. C. K.; Tong, S. Y.; Lee, S. T. *Science* **2003**, *299*, 1874.
- (2) (a) Fennimore, A. M.; Yuzvinsky, T. D.; Han, W. Q.; Fuhrer, M. S.; Cumings, J.; Zettl, A. *Nature* **2003**, *424*, 408. (b) Zhong, Z.; Wang, D.; Cui, Y.; Bockrath, M. W.; Lieber, C. M. *Science* **2003**, *302*, 1377.
- (3) (a) Hu, J. Q.; Bando, Y.; Zhan, J. H.; Golberg, D. *Angew. Chem., Int. Ed.* **2004**, *43*, 4606. (b) Shen, G. Z.; Bando, Y.; Lee, C. J. *J. Phys. Chem. B* **2005**, *109*, 10578.
- (4) Sze, S. M. *Physics of Semiconductor Devices*; Wiley-Interscience: New York, NY, 1981. (b) Gudiksen, M. S.; Lauhon, L. J.; Wang, J.; Smith, D. C.; Lieber, C. M. *Nature* **2002**, *415*, 617.
- (5) (a) Iijima, S. *Nature* **1991**, *354*, 56. (b) Nath, M.; Rao, C. N. R. *Angew. Chem., Int. Ed.* **2002**, *41*, 3451. (c) Dai, H. *Acc. Chem. Res.* **2002**, *35*, 1035.
- (6) Han, W. Q.; Zettl, A. *Appl. Phys. Lett.* **2002**, *81*, 5051.
- (7) (a) Hu, J. Q.; Bando, Y.; Liu, Z. W.; Zhan, J. H.; Golberg, D.; Sekiguchi, T. *Angew. Chem., Int. Ed.* **2004**, *43*, 63. (b) Tang, C. C.; Bando, Y.; Golberg, D.; Ma, R. Z. *Angew. Chem., Int. Ed.* **2005**, *44*, 576.
- (8) Duan, X.; Huang, Y.; Cui, Y.; Wang, J.; Lieber, C. M. *Nature* **2001**, *409*, 66.
- (9) (a) Pan, Z. W.; Dai, Z. R.; Wang, Z. L. *Science* **2001**, *291*, 1947. (b) Lee, S. T.; Wang, N.; Zhang, Y. F.; Tang, Y. H. *MRS Bull.* **1999**, *24*, 36. (c) Chen, D.; Tang, K. B.; Liang, Z. H.; Liu, Y. K.; Zheng, H. G. *Nanotechnology* **2005**, *16*, 2619.
- (10) Pentes, V. F.; Zanchet, D.; Erdonmez, C. K.; Alivisatos, A. P. *J. Am. Chem. Soc.* **2002**, *124*, 12874.
- (11) Xia, Y. N.; Yang, P. D.; Sun, Y.; Wu, Y.; Mayers, B.; Gates, B.; Yin, Y.; Kim, F.; Yan, H. *Adv. Mater.* **2003**, *15*, 353.
- (12) (a) Korgel, A. B.; Fitzmaurice, D. *Adv. Mater.* **1998**, *10*, 661. (b) Trentler, T. J.; Hickman, K. M.; Goel, S. C.; Viano, A. M.; Gibbons, P. C.; Buhro, W. M. *Science* **1995**, *270*, 1791. (c) Cho, K.; Talapin, D. V.; Gaschler, W.; Murray, C. B. *J. Am. Chem. Soc.* **2005**, *127*, 7140.
- (13) (a) Hu, J. T.; Ouyang, M.; Yang, P. D.; Lieber, C. M. *Nature* **1999**, *399*, 48. (b) Cui, Y.; Lieber, C. M. *Science* **2001**, *291*, 851. (c) Lieber, C. M. *Nano Lett.* **2002**, *2*, 81. (d) Lauhon, L. J.; Gudiksen, M. S.; Wang, D. L.; Lieber, C. M. *Nature* **2002**, *420*, 57.
- (14) (a) Wu, Y.; Fan, R.; Yang, P. D. *Nano Lett.* **2002**, *2*, 83. (b) Li, Y.; Ye, C. H.; Fang, X. S.; Yang, L.; Xiao, Y. H.; Zhang, L. D. *Nanotechnology* **2005**, *16*, 501.
- (15) (a) Bjork, M. T.; Ohlsson, B. J.; Sass, T.; Persson, A. I.; Thelander, C.; Magnusson, K.; Deppert, M. H.; Wallenberg, L.; Samuelson, L. *Nano Lett.* **2002**, *2*, 87. (b) Manna, L.; Scher, E. C.; Li, L. S.; Alivisatos, A. P. *J. Am. Chem. Soc.* **2002**, *124*, 7136.
- (16) (a) Hu, J. Q.; Bando, Y.; Liu, Z.; Sekiguchi, T.; Golberg, D.; Zhan, J. *J. Am. Chem. Soc.* **2003**, *125*, 11306. (b) Zhan, J. H.; Bando, Y.; Hu, J. Q.; Liu, Z. W.; Golberg, D. *Angew. Chem., Int. Ed.* **2005**, *44*, 2140.
- (17) (a) Ye, C. H.; Zhang, L. D.; Fang, X. S.; Wang, Y.; Yan, P.; Zhao, J. *Adv. Mater.* **2004**, *16*, 1019. (b) Li, Q.; Wang, C. R. *J. Am. Chem. Soc.* **2003**, *125*, 9892.
- (18) (a) Wang, X. D.; Song, J. H.; Li, P.; Ryou, J. H.; Dupuis, R. D.; Summers, C. J.; Wang, Z. L. *J. Am. Chem. Soc.* **2005**, *127*, 7920.
- (19) (a) Lao, J. Y.; Wen, J. G.; Ren, Z. F. *Nano Lett.* **2002**, *2*, 1287. (b) Bae, S. Y.; Seo, H. W.; Choi, H. C.; Park, J. J. *Phys. Chem. B* **2004**, *108*, 12318.
- (20) (a) Hu, J. Q.; Bando, Y.; Zhan, J. H.; Yuan, X. L.; Sekiguchi, T.; Golberg, D. *Adv. Mater.* **2005**, *17*, 971. (b) Zhu, Y. C.; Bando, Y.; Yin, L. W. *Adv. Mater.* **2004**, *16*, 331. (c) H. Wang, X. H. Zhang, X. M. Meng, S. M. Zhou, S. K. Wu, W. S. Shi, S. T. Lee, *Angew. Chem., Int. Ed.* **2005**, *44*, 6934.
- (21) (a) Golberg, D.; Bando, Y.; Bourgeois, L.; Kurashima, K.; Sato, T. *Carbon* **2000**, *38*, 2017. (b) Han, W.; Bando, Y.; Kurashima, K.; Sato, Y. *Appl. Phys. Lett.* **1998**, *73*, 3085.
- (22) (a) Wagner, R. S.; Ellis, W. C. *Appl. Phys. Lett.* **1964**, *4*, 89. (b) Sears, G. W. *Acta Metall. Sin.* **1956**, *3*, 268.
- (23) Pan, Z. W.; Dai, Z. R.; Ma, C.; Wang, Z. L. *J. Am. Chem. Soc.* **2002**, *124*, 1817.
- (24) (a) Yin, L. W.; Bando, Y.; Zhan, J. H.; Li, M. S.; Golberg, D. *Adv. Mater.* **2005**, *17*, 1972. (b) Ye, C. H.; Fang, X. S.; Li, G. H.; Zhang, L. D. *Appl. Phys. Lett.* **2004**, *85*, 3035. (c) Hu, J. Q.; Bando, Y.; Zhan, J. H.; Golberg, D. *Adv. Funct. Mater.* **2005**, *15*, 757.